Photolithography-based Fabrication of Interdigitated Electrodes with Integrated Gold Microheater: Temperature Distribution Study

Milena Rašljić Rafajilović, Marko Bošković, Milija Sarajlić, Ivana Mladenović, Ivan Pešić, Dana Vasiljević-Radović, *Member, IEEE,* Marija V. Pergal

Abstract— **Interdigitated electrodes with integrated heaters fabricated on a Si platform were investigated in this study. The electrodes and heaters were made of gold, using standard photolithography processes. The primary objective was to analyze the maximum temperature achievable on the microheater and characterize its temperature distribution. The integrated heater achieved a maximum temperature of 420 °C with an applied voltage of 16 V. The temperature distribution was uniform across the entire surface of the heater, which was located on the underside of the chip beneath the interdigitated electrodes. At higher temperatures, the silver paste, utilized as a bonding agent between the copper wires and heater, underwent melting.**

Index Terms—**microheater, interdigitated electrodes, sensors, temperature, photolithography**

I. Introduction

Interdigital sensors are widely used in various fields, including sensing, biology, environmental and industrial applications. They consist of interdigitated electrodes which are periodically placed on platform, and they can be covered with a thick layer of conducting material, most commonly metals, resulting in a comb-shaped arrangement or zipper-like structure [1, 2]. The first interdigitated electrodes were patented by N. Tesla in 1891 [3], and theoretical calculations of capacitance between planar strips were published in the 1920s [4]. In the 1960s, interdigitated electrodes became widely used in sensing applications [5, 6].

Nowadays there is wide spectra of use interdigitated electrodes such as tunable devices, surface acoustic wave devices [7], acoustic transducers [8], chemical sensors, humidity sensors, CO_2 sensors [9-11], in biology [12], environmental and industry application [13].

Interdigitated electrodes offer several advantages, such as scaling down the dimensions of electrodes and distances between them, low cost, and a wide range of potential uses without changing the structure design. They provide increased signal-to-noise ratio, low ohmic drop, and a fast response time to reach a steady state [14]. Additionally, the design of interdigitated electrodes eliminates the need for a reference electrode and provides a simple and fast steady-state current response.

Different types of materials can be used for the platforms of these devices, such as polymers [15, 16], ceramics [17], glass [18], and silicon [2]. The choice of material depends on the specific application and materials can be either flexible or rigid [1].

Heaters are crucial components of interdigital sensors, and their size, position, and material are important factors in the design and fabrication of these devices, such as interdigital sensors [11, 17]. In this study, we used silicon (Si) as the platform for interdigitated electrodes and heaters, and gold (Au) as the material of choice for their fabrication. Standard photolithography processes were employed for their fabrication. Our device will be used as a humidity sensor, and our goal was to demonstrate the thermal distribution on the heater and obtain a temperature higher than 100 °C.

II. The Method

We used a 3-inch diameter, 380 µm thick, double-sided polished, n-type silicon (Si) wafer with a resistivity of 3-5 Ωcm as the platform for our heater and interdigitated electrodes. We grew a silicon dioxide (SiO_2) layer on both sides of the Si substrate in an oxidation furnace as an insulating layer between the metal and the Si substrate. The thermal oxide was obtained at a temperature of 1100°C, and the thickness of that layer was 0.6 µm. After oxidation, we sputtered gold (Au) with a sublayer of chromium (Cr) in a *Perkin Elmer 2400 sputtering system* on both sides of the Si

Milena Rašljić Rafajilović, Institute of Chemistry, Technology and Metallurgy, Centre for Microelectronic Technologies, University of Belgrade, 11000Belgrade, Serbia (e-mail: milena@nanosys.ihtm.bg.ac.rs), (https://orcid.org/0000-0001-8170-746X)

Marko Bošković, Institute of Chemistry, Technology and Metallurgy, Centre for Microelectronic Technologies, University of Belgrade, 11000 Belgrade, Serbia (e-mail: boskovic@nanosys.ihtm.bg.ac.rs), (https://orcid.org/0000-0003-1428-9346)

Milija Sarajlić, Institute of Chemistry, Technology and Metallurgy, Centre for Microelectronic Technologies, University of Belgrade, 11000Belgrade, Serbia (e-mail: milijas@nanosys.ihtm.bg.ac.rs), (https://orcid.org/0000-0002-1267-1827)

Ivana Mladenović, Institute of Chemistry, Technology and Metallurgy, Centre for Microelectronic Technologies, University of Belgrade, 11000 Belgrade, Serbia (e-mail: ivana@nanosys.ihtm.bg.ac.rs), (https://orcid.org/0000-0002-6852-7541)

Ivan Pešić, Institute of Chemistry, Technology and Metallurgy, Centre for Microelectronic Technologies, University of Belgrade, 11000 Belgrade, Serbia (e-mail: ipesic@nanosys.ihtm.bg.ac.rs), (https://orcid.org/0000-0002-2124-7139)

Dana Vasiljević-Radović, Institute of Chemistry, Technology and Metallurgy, Centre for Microelectronic Technologies, University of Belgrade, 11000 Belgrade, Serbia (e-mail: dana@nanosys.ihtm.bg.ac.rs), (https://orcid.org/0000-0002-7609-8599)

Marija V. Pergal, Institute of Chemistry, Technology and Metallurgy, Centre for Microelectronic Technologies, University of Belgrade, 11000 Belgrade, Serbia (e-mail: marija.pergal@ihtm.bg.ac.rs), (https://orcid.org/0000-0001-6078-2006)

 ISBN 978-86-7466-970-9

substrate. The sublayer of chromium was used to improve the adhesion of Au on SiO_2. Both layers were sputtered in an atmosphere of argon (Ar) at a pressure value of 17 mTorr but with different parameters. The RF power for Au sputtering was 150 W for 10 min, and for Cr, it was 250 W for 5 min. At the end, the thickness of Cr was 10 nm, and the thickness of Au was 150 nm. Figure 1 presents a schematic view of all the fabrication steps of the integrated heater and interdigitated electrodes on the Si substrate.

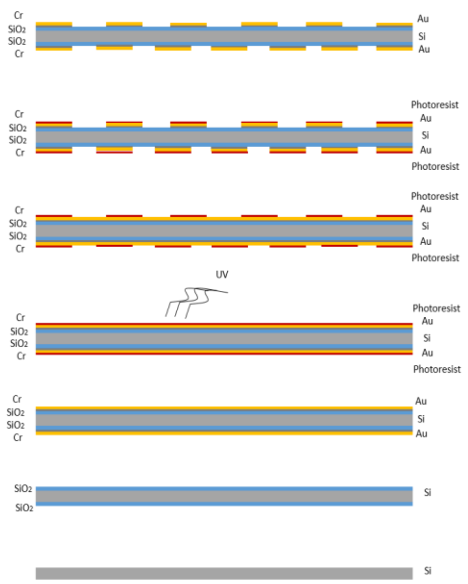

Fig. 1. Schematic view of fabrication steps of heater and interdigital electrodes

Before the sputtering process, the wafers were treated with appropriate solutions to obtain a clean Si surface. The first step was treatment with Piranha solution (sulfuric acid and hydrogen peroxide in a 3:1 ratio) at 100 °C, and the second step was treatment in a hydrochloric acid solution with hydrogen peroxide (1:1 ratio) at 70 °C. The aim of these treatments was to clean substrates of organic and inorganic residues. After oxidation, cleaning steps, and sputtering processes, the substrate was ready for standard photolithography steps. We applied photoresist on both sides of the wafer, using commercial photoresists, AZ 1518 and AZ1505, with thicknesses of 1.8 µm and 0.5 µm, respectively. At the end, the total thickness of the photoresist was 2.3 µm.

In the first step, the photoresist on the top side was used to transfer patterns from masks on the top side of the substrate, while the photoresist on the bottom side of the wafer served to protect the gold layer on the bottom side from mechanical damage. We used a laser writer (*LW405*) to transfer the patterns from the mask to the substrate. After exposure of the photoresist, the gold and chromium layers were etched in a solution to obtain interdigitated electrodes on the top side of the wafer. The photoresist was then removed with acetone, and the wafer was ready for the next photolithography step.

In the next step, we applied photoresist on both sides of the wafer again. In this step, the photoresist on the top side of the wafer served as a protecting layer from mechanical damage for the formed patterns, and the bottom photoresist had the role of transferring patterns from the mask on the substrate. We obtained heaters on the bottom side of the substrate, under the interdigitated electrodes, using this step. After photoresist exposure, the Au and Cr on the bottom side were etched, and then the photoresist was removed with acetone from both sides. As a result, we obtained interdigitated electrodes and a microheater of Au on the Si substrate as the platform.

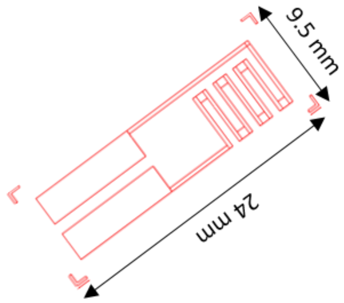

Fig. 2. Masks of microheater

After the photolithography processes, the wafer was cut resulting in a single chip with dimensions of 24 mm x 9.5 mm, as shown in Figure 2. The interdigitated electrodes made of gold were located on the top side of the chip, as illustrated in Figure 3.a. On the bottom side of the chip, the microheater made of the same material was located, as shown in Figure 3.b. The heater had dimensions of 300 µm in diameter and 57.9 mm in length.

a) b)

Fig. 3. Fabricated sensor with integrated microheater a) top side with interdigitated electrodes, b) bottom side with heater

III. MAIN RESULTS

After fabrication, the microheater was connected to the voltage source. Experimental setup is shown in Figure 4. Copper wires were utilized to connect the microheater to the voltage source using silver paste. The *BK Precision 9714b source* was utilized as the voltage source, and the Infra-Red Camera *FLIR E5* was employed for temperature measurements. The chip, which included the interdigitated electrodes and microheater, was placed in a dark chamber with minimal air flow, with an ambient temperature of 22 °C. The emissivity was measured at 0.3, and the distance of the IR Camera from the sample was 15 cm.

 ISBN 978-86-7466-970-9

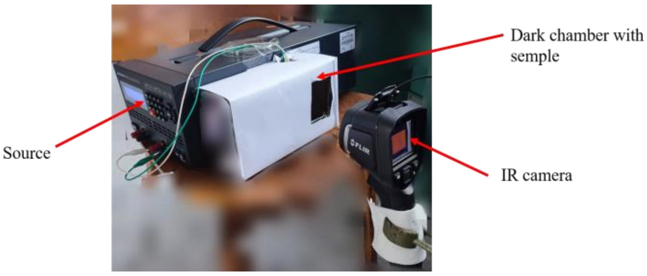

Fig. 4. Experimental setting for temperature measurements

The resistance of the microheater was 31.8 Ω at ambient temperature. Different voltage values were applied, ranging from 1 V to 16 V. Influence of applied voltage and power on heater's temperature is shown in Figures 5 and 6. The temperature increased almost exponentially within the applied voltage range, while the temperature-power dependence was linear up to 4 W. The difference in trends in temperature *versus* voltage and temperature *versus* power curves was attributed to the change in the microheater's resistance with temperature, as shown in Figure 7.

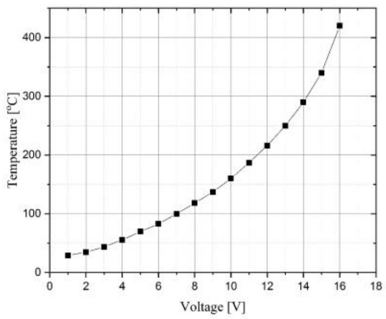

Fig. 5. Temperature versus applied voltage

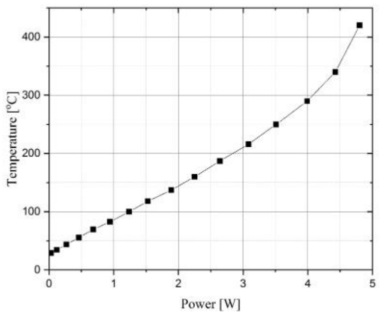

Fig. 6. Temperature versus applied power

At the maximum voltage value of 16 V, the measured temperature was 420 °C, which was the highest temperature achieved on the integrated heater. The silver paste began to lose its performance at temperatures above 420 °C, serving as a limiting factor that prevented higher temperatures from being achieved.

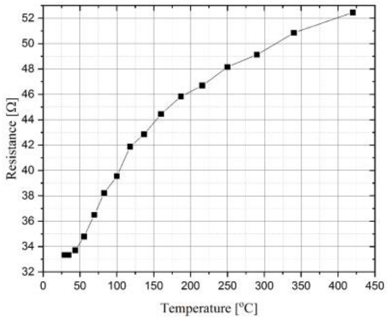

Fig. 7. Temperature dependence of resistivity

At 10 V, the maximum temperature reached was 180 °C, which was more than sufficient for use in interdigitated sensors. Figure 8 depicts that the temperature reached a stationary state after 1 minute.

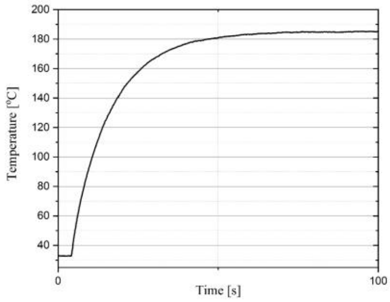

Fig. 8. Temperature change trough time for voltage of 10 V

Following these experiments, the temperature distribution on the surface of the microheater was examined, and the results were compared with simulation results. The microheater was simulated using Comsol Multiphysics, utilizing the Heat Transfer and Electric Current modules. The material properties required for simulation are given in Table 1.

Table 1. The material properties required for simulation.

	Electrical conductivity [S/m]	**Heat capacity [J/(kg·K)]**	**Thermal conductivity [W/(m·K)]**
Gold	45.6×10^{6}	129	317
Silicon	25	700	130
Silicon dioxide	1×10^{-12}	730	1.4

A constant voltage of 10 V was applied to the heater's electrical contact, and the simulation results were compared with the experimental results in the stationary state of the heater (Figure 9). In Figure 9a), it was demonstrated that the maximum temperature on the heater reached 183.5 °C and the temperature distribution was uniform at the center of the microheater, decreasing towards the edges of the chip. Additionally, the results of the simulated system were shown to be compatible with the fabricated structure, as seen in Figure 9b.

 ISBN 978-86-7466-970-9

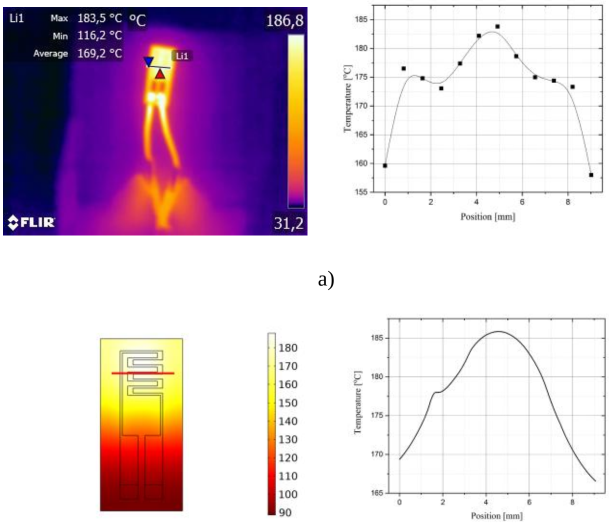

a)

b)

Fig. 9. Temperature distribution on microheater surface a) experimental results, b) simulation results

IV. CONCLUSION

In this study, we have presented the fabrication process of microheaters integrated with interdigitated electrodes on a silicon substrate. Both the heater and interdigitated electrodes were made of gold. Our experimental and simulation results have shown that the temperature distribution on the microheater surface was uniform. We achieved a maximum temperature of 420 °C on the integrated heater by applying a voltage of 16 V. However, the limiting factor for achieving higher temperatures was the silver paste used, which melted at higher temperatures. Furthermore, we have demonstrated good compatibility between the experimental and simulation results regarding temperature distribution on the heater surface. In our future work, we aim to examine different types of bonds for copper wires to achieve higher temperatures, as well as to investigate the use of different materials for interdigitated electrodes and heaters.

ACKNOWLEDGMENT

This research has been financially supported by the Ministry of Science, Technological Development, and Innovation of Republic of Serbia (Contract No: 451-03-47/2023-01/200026).

REFERENCES

[1] A. V. Mamishev, K. Sundara-Rajan, Y. Fumin, D. Yanqing, and M. Zahn, “Interdigital sensors and transducers,” *Proceedings of the IEEE,* vol. 92, no. 5, pp. 808-845, 2004.

[2] M. V. Bošković, B. Šljukić, D. Vasiljević Radović, K. Radulović, M. Rašljić Rafajilović, M. Frantlović, and M. Sarajlić, “Full-self-powered humidity sensor based on electrochemical aluminum–water reaction,” *Sensors,* vol. 21, no. 10, pp. 3486, 2021.

[3] N. Tesla, *Electric condenser*, 464 667, 1891.

[4] A. E. H. Love, “Some electrostatic distributions in two dimensions,” *Proceedings of the London Mathematical Society,* vol. 2, no. 1, pp. 337-369, 1924.

[5] W. S. Mortley, “Pulse compression by dispersive gratings on crystal quartz(Pulse compression by dispersive gratings on crystal quartz, describing ultrasonic method and wave transformation of frequency-swept radar pulses),” *Marconi Review,* vol. 28, pp. 273-290, 1965.

[6] I. G. Matis, “On multiparameter control of dielectric properties of laminate polymer materials,” *Latvijas PSR Zinatnu Akademijas Vestis Fizikas un Tehnisko,* vol. 6, pp. 60-67, 1966.

[7] M.-I. Rocha-Gaso, C. March-Iborra, Á. Montoya-Baides, and A. Arnau-Vives, “Surface generated acoustic wave biosensors for the detection of pathogens: A review,” *Sensors,* vol. 9, no. 7, pp. 5740-5769, 2009.

[8] N. A. Ramli, and A. N. Nordin, "Design and modeling of MEMS SAW resonator on Lithium Niobate." pp. 1-4.

[9] M. Kitsara, D. Goustouridis, S. Chatzandroulis, M. Chatzichristidi, I. Raptis, T. Ganetsos, R. Igreja, and C. J. Dias, “Single chip interdigitated electrode capacitive chemical sensor arrays,” *Sensors and Actuators B: Chemical,* vol. 127, no. 1, pp. 186-192, 2007.

[10] M. Sarajlić, M. V. Bošković, S. Andrić, J. N. Stevanović, M. Spasenović, and I. Jokić, "Humidity and CO2 Sensing Using a Graphene Film-Based Sensor Obtained by Using Liquid-Phase Exfoliation," *Engineering Proceedings,* 21, 2022].

[11] S. Andrić, T. Tomašević-Ilić, M. V. Bošković, M. Sarajlić, D. Vasiljević-Radović, M. M. Smiljanić, and M. Spasenović, “Ultrafast humidity sensor based on liquid phase exfoliated graphene,” *Nanotechnology,* vol. 32, no. 2, pp. 025505, 2020/10/14, 2021.

[12] M. Ibrahim, J. Claudel, D. Kourtiche, and M. Nadi, “Geometric parameters optimization of planar interdigitated electrodes for bioimpedance spectroscopy,” *Journal of Electrical Bioimpedance,* vol. 4, no. 1, pp. 13-22, 2013.

[13] N. Afsarimanesh, A. Nag, M. E. E. Alahi, T. Han, and S. C. Mukhopadhyay, “Interdigital sensors: Biomedical, environmental and industrial applications,” *Sensors and Actuators A: Physical,* vol. 305, pp. 111923, 2020.

[14] S. Ding, “Highly sensitive biosensors with interdigitated electrode arrays,” 2018.

[15] P. Zaccagnini, C. Ballin, M. Fontana, M. Parmeggiani, S. Bianco, S. Stassi, A. Pedico, S. Ferrero, and A. Lamberti, “Laser-Induced Graphenization of PDMS as Flexible Electrode for Microsupercapacitors,” *Advanced Materials Interfaces,* vol. 8, no. 23, pp. 2101046, 2021.

[16] L. Liu, Y. Xu, F. Cui, Y. Xia, L. Chen, X. Mou, and J. Lv, “Monitoring of bacteria biofilms forming process by in-situ impedimetric biosensor chip,” *Biosensors and Bioelectronics,* vol. 112, pp. 86-92, 2018/07/30/, 2018.

[17] J. N. Stevanović, S. P. Petrović, N. B. Tadić, K. Cvetanović, A. G. Silva, D. V. Radović, and M. Sarajlić, "Mechanochemical Synthesis of TiO2-CeO2 Mixed Oxides Utilized as a Screen-Printed Sensing Material for Oxygen Sensor," *Sensors,* 23, 2023].

[18] M.-S. Wu, W.-C. Shih, and W.-H. Tsai, “Growth of ZnO thin films on interdigital transducer/Corning 7059 glass substrates by two-step fabrication methods for surface acoustic wave applications,” *Journal of Physics D: Applied Physics,* vol. 31, no. 8, pp. 943, 1998.